

Search for Dark Matter Annihilation Signals in the H.E.S.S. Inner Galaxy Survey

H. Abdalla,¹ F. Aharonian,^{2,3,4} F. Ait Benkhali,³ E. O. Angüner,⁵ C. Armand,⁶ H. Ashkar,⁷ M. Backes,^{1,8} V. Baghmanyany,⁹ V. Barbosa Martins,¹⁰ R. Batzofin,¹¹ Y. Becherini,¹² D. Berge,¹⁰ K. Bernlöhr,³ B. Bi,¹³ M. Böttcher,⁸ J. Bolmont,¹⁴ M. de Bony de Lavergne,⁶ R. Brose,² F. Brun,⁷ F. Cangemi,¹⁴ S. Caroff,¹⁴ M. Cerruti,¹⁵ T. Chand,⁸ A. Chen,¹¹ G. Cotter,¹⁶ J. Damascene Mbarubucyeye,¹⁰ J. Devin,¹⁷ A. Djannati-Atai,¹⁵ A. Dmytriiev,¹⁸ V. Doroshenko,¹³ K. Egberts,¹⁹ A. Fiasson,⁶ G. Fichet de Clairfontaine,¹⁸ G. Fontaine,²⁰ S. Funk,²¹ S. Gabici,¹⁵ G. Giavitto,¹⁰ D. Glawion,²¹ J. F. Glicenstein,⁷ M.-H. Grondin,¹⁷ J. A. Hinton,³ W. Hofmann,³ T. L. Holch,¹⁰ M. Holler,²² D. Horns,²³ Zhiqiu Huang,³ M. Jamrozy,²⁴ F. Jankowsky,²⁵ E. Kasai,¹ K. Katarzyński,²⁶ U. Katz,²¹ B. Khélifi,¹⁵ W. Kluźniak,²⁷ Nu. Komin,¹¹ K. Kosack,⁷ D. Kostunin,¹⁰ G. Lamanna,⁶ M. Lemoine-Goumard,¹⁷ J.-P. Lenain,¹⁴ F. Leuschner,¹³ T. Lohse,²⁸ A. Luashvili,¹⁸ I. Lypova,²⁵ J. Mackey,² D. Malyshev,^{13,*} D. Malyshev,²¹ V. Marandon,³ P. Marchegiani,¹¹ G. Martí-Devesa,²² R. Marx,²⁵ G. Maurin,⁶ M. Meyer,²¹ A. Mitchell,³ R. Moderski,²⁷ A. Montanari,^{7,*} E. Moulin,^{7,*} J. Muller,²⁰ M. de Naurois,²⁰ J. Niemiec,⁹ A. Priyana Noel,²⁴ S. Ohm,¹⁰ L. Olivera-Nieto,³ E. de Ona Wilhelmi,¹⁰ M. Ostrowski,²⁴ S. Panny,²² M. Panter,³ R. D. Parsons,²⁸ G. Peron,³ V. Poireau,⁶ H. Prokoph,¹⁰ G. Pühlhofer,¹³ M. Punch,^{15,12} A. Quirrenbach,²⁵ P. Reichherzer,⁷ A. Reimer,²² O. Reimer,²² M. Renaud,²⁹ F. Rieger,³ G. Rowell,³⁰ B. Rudak,²⁷ H. Rueda Ricarte,⁷ E. Ruiz-Velasco,³ V. Sahakian,³¹ H. Salzmann,¹³ A. Santangelo,¹³ M. Sasaki,²¹ F. Schüssler,⁷ H. M. Schutte,⁸ U. Schwanke,²⁸ M. Senniappan,¹² J. N. S. Shapopi,¹ H. Sol,¹⁸ A. Specovius,²¹ S. Spencer,¹⁶ Ł. Stawarz,²⁴ C. Stegmann,^{19,10} S. Steinmassl,³ C. Steppa,¹⁹ T. Takahashi,³² T. Tanaka,³³ R. Terrier,¹⁵ C. Thorpe-Morgan,¹³ M. Tluczykont,²³ M. Tsirou,³ N. Tsuji,³⁴ Y. Uchiyama,³⁵ C. van Eldik,²¹ J. Veh,²¹ J. Vink,³⁶ S. J. Wagner,²⁵ R. White,³ A. Wiercholska,⁹ Yu Wun Wong,²¹ M. Zacharias,¹⁸ D. Zargaryan,^{2,4} A. A. Zdziarski,²⁷ A. Zech,¹⁸ S. J. Zhu,¹⁰ S. Zouari,¹⁵ and N. Żywucka⁸

(H.E.S.S. Collaboration)

¹University of Namibia, Department of Physics, Private Bag 13301, Windhoek 10005, Namibia²Dublin Institute for Advanced Studies, 31 Fitzwilliam Place, D02 XF86 Dublin 2, Ireland³Max-Planck-Institut für Kernphysik, P.O. Box 103980, D 69029 Heidelberg, Germany⁴High Energy Astrophysics Laboratory, RAU, 123 Hovsep Emin St Yerevan 0051, Armenia⁵Aix Marseille Université, CNRS/IN2P3, CPPM, Marseille, France⁶Université Savoie Mont Blanc, CNRS, Laboratoire d'Annecy de Physique des Particules—IN2P3, 74000 Annecy, France⁷IRFU, CEA, Université Paris-Saclay, F-91191 Gif-sur-Yvette, France⁸Centre for Space Research, North-West University, Potchefstroom 2520, South Africa⁹Instytut Fizyki Jądrowej PAN, ulica Radzikowskiego 152, 31-342 Kraków, Poland¹⁰DESY, D-15738 Zeuthen, Germany¹¹School of Physics, University of the Witwatersrand, 1 Jan Smuts Avenue, Braamfontein, Johannesburg, 2050 South Africa¹²Department of Physics and Electrical Engineering, Linnaeus University, 351 95 Växjö, Sweden¹³Institut für Astronomie und Astrophysik, Universität Tübingen, Sand 1, D 72076 Tübingen, Germany¹⁴Sorbonne Université, Université Paris Diderot, Sorbonne Paris Cité, CNRS/IN2P3,

Laboratoire de Physique Nucléaire et de Hautes Energies, LPNHE, 4 Place Jussieu, F-75252 Paris, France

¹⁵Université de Paris, CNRS, Astroparticule et Cosmologie, F-75013 Paris, France¹⁶University of Oxford, Department of Physics, Denys Wilkinson Building, Keble Road, Oxford OX1 3RH, United Kingdom¹⁷Université Bordeaux, CNRS/IN2P3, Centre d'Études Nucléaires de Bordeaux Gradignan, 33175 Gradignan, France¹⁸Laboratoire Univers et Théories, Observatoire de Paris, Université PSL, CNRS, Université de Paris, 92190 Meudon, France¹⁹Institut für Physik und Astronomie, Universität Potsdam, Karl-Liebknecht-Strasse 24/25, D 14476 Potsdam, Germany²⁰Laboratoire Leprince-Ringuet, École Polytechnique, CNRS, Institut Polytechnique de Paris, F-91128 Palaiseau, France²¹Friedrich-Alexander-Universität Erlangen-Nürnberg, Erlangen Centre for Astroparticle Physics, Erwin-Rommel-Str. 1, D 91058 Erlangen, Germany²²Institut für Astro- und Teilchenphysik, Leopold-Franzens-Universität Innsbruck, A-6020 Innsbruck, Austria²³Universität Hamburg, Institut für Experimentalphysik, Luruper Chaussee 149, D 22761 Hamburg, Germany²⁴Observatorium Astronomiczne, Uniwersytet Jagielloński, ulica Orła 171, 30-244 Kraków, Poland²⁵Landessternwarte, Universität Heidelberg, Königstuhl, D 69117 Heidelberg, Germany²⁶Institute of Astronomy, Faculty of Physics, Astronomy and Informatics, Nicolaus Copernicus University, Grudziadzka 5, 87-100 Torun, Poland²⁷Nicolaus Copernicus Astronomical Center, Polish Academy of Sciences, ulica Bartycka 18, 00-716 Warsaw, Poland²⁸Institut für Physik, Humboldt-Universität zu Berlin, Newtonstrasse 15, D 12489 Berlin, Germany

²⁹Laboratoire Univers et Particules de Montpellier, Université Montpellier, CNRS/IN2P3, CC 72, Place Eugène Bataillon, F-34095 Montpellier Cedex 5, France

³⁰School of Physical Sciences, University of Adelaide, Adelaide 5005, Australia

³¹Yerevan Physics Institute, 2 Alikhanian Brothers Street 375036 Yerevan, Armenia

³²Kavli Institute for the Physics and Mathematics of the Universe (WPI), The University of Tokyo Institutes for Advanced Study (UTIAS), The University of Tokyo, 5-1-5 Kashiwa-no-Ha, Kashiwa, Chiba, 277-8583, Japan

³³Department of Physics, Konan University, 8-9-1 Okamoto, Higashinada, Kobe, Hyogo 658-8501, Japan

³⁴RIKEN, 2-1 Hirosawa, Wako, Saitama 351-0198, Japan

³⁵Department of Physics, Rikkyo University, 3-34-1 Nishi-Ikebukuro, Toshima-ku, Tokyo 171-8501, Japan

³⁶GRAPPA, Anton Pannekoek Institute for Astronomy, University of Amsterdam, Science Park 904, 1098 XH Amsterdam, Netherlands



(Received 11 October 2021; revised 17 January 2022; accepted 13 July 2022; published 8 September 2022)

The central region of the Milky Way is one of the foremost locations to look for dark matter (DM) signatures. We report the first results on a search for DM particle annihilation signals using new observations from an unprecedented γ -ray survey of the Galactic Center (GC) region, i.e., the Inner Galaxy Survey, at very high energies ($\gtrsim 100$ GeV) performed with the H.E.S.S. array of five ground-based Cherenkov telescopes. No significant γ -ray excess is found in the search region of the 2014–2020 dataset and a profile likelihood ratio analysis is carried out to set exclusion limits on the annihilation cross section $\langle\sigma v\rangle$. Assuming Einasto and Navarro-Frenk-White (NFW) DM density profiles at the GC, these constraints are the strongest obtained so far in the TeV DM mass range. For the Einasto profile, the constraints reach $\langle\sigma v\rangle$ values of $3.7 \times 10^{-26} \text{ cm}^3 \text{ s}^{-1}$ for 1.5 TeV DM mass in the W^+W^- annihilation channel, and $1.2 \times 10^{-26} \text{ cm}^3 \text{ s}^{-1}$ for 0.7 TeV DM mass in the $\tau^+\tau^-$ annihilation channel. With the H.E.S.S. Inner Galaxy Survey, ground-based γ -ray observations thus probe $\langle\sigma v\rangle$ values expected from thermal-relic annihilating TeV DM particles.

DOI: [10.1103/PhysRevLett.129.111101](https://doi.org/10.1103/PhysRevLett.129.111101)

Introduction.—The total matter content of the Universe is made of about 85% dark and nonbaryonic matter as suggested by growing evidence from astrophysics and cosmology [1,2]. However, the nature of the dark matter (DM) remains a fundamental question of modern physics. A compelling class of stable DM candidates are weakly interacting massive particles (WIMPs) [3–5]. Such particles with mass and coupling strength at the electroweak scale naturally emerge in several extensions of the standard model of particle physics. WIMPs are thermally produced in the early Universe and their relic density can represent all the DM in the Universe [6], as accurately measured from cosmological observations. The quest for WIMPs motivates numerous experimental efforts to probe their non-gravitational properties such as their production at particle colliders [7], their scattering off nuclei on Earth [8], and their decay and annihilation [9].

WIMPs would self-annihilate today in dense astrophysical environments, producing gamma rays in the final state from hadronization, radiation, and decay of the standard model particles produced in the annihilation process. Such gamma rays could be eventually detected by ground-based arrays of Imaging Atmospheric Cherenkov Telescopes (IACTs) such as the High Energy Stereoscopic System (H.E.S.S.) provided that the WIMP mass is high enough. The self-annihilation of Majorana WIMPs of mass m_{DM} would produce an energy-differential flux of gamma rays in a solid angle $\Delta\Omega$ expressed as

$$\frac{d\Phi_\gamma}{dE_\gamma}(E_\gamma, \Delta\Omega) = \frac{\langle\sigma v\rangle}{8\pi m_{\text{DM}}^2} \sum_f BR_f \frac{dN_\gamma^f}{dE_\gamma}(E_\gamma) J(\Delta\Omega)$$

$$\text{with } J(\Delta\Omega) = \int_{\Delta\Omega} \int_{\text{los}} \rho^2[s(r, \theta)] ds d\Omega. \quad (1)$$

$\langle\sigma v\rangle$ is the velocity-weighted annihilation cross section averaged over the velocity distribution and dN_γ^f/dE_γ is the differential yield of gamma rays per annihilation in the channel f with its branching ratio BR_f . The term $J(\Delta\Omega)$, hereafter referred to as the J factor, corresponds to the integral of the square of the DM density ρ over the line of sight s and solid angle $\Delta\Omega$. The DM density ρ is assumed spherically symmetric and therefore depends only on the radial coordinate r from the center of the DM halo. It can be expressed as $r = (s^2 + r_\odot^2 - 2r_\odot s \cos\theta)^{1/2}$, with r_\odot the distance of the observer to the GC taken to be $r_\odot = 8.5$ kpc [10], and θ the angle between the direction of observation and the Galactic Center. The center of the Milky Way is predicted as the brightest source of DM annihilations with a DM distribution assumed to follow cuspy profiles conveniently described by the Einasto [11] or Navarro-Frenk-White [12] parametrizations. Commonly used sets of parameters for the above-mentioned DM profiles [13,14] considered here are given in Table II of Ref. [15]. The DM profiles are normalized to the local DM density ρ_\odot such that $\rho(r_\odot) = \rho_\odot = 0.39 \text{ GeV cm}^{-3}$ [17]. Improved determinations of the local DM density are being carried out

(see, for instance, Ref. [18,19]). A change of ρ_{\odot} can be propagated to the results by rescaling the DM signal by $(\rho_{\odot}/0.39 \text{ GeV cm}^{-3})^2$. Other parametrizations such as the Burkert [21] or Moore [22] profile can be used. However, cored profiles such as the Burkert one are not studied here, since they need dedicated observations and analysis procedures [23]. The strongest constraints so far obtained on WIMPs in the TeV mass range come from 254 h of H.E.S.S. observations of the Galactic Center region [13]. In the present work, about 5 times more exposure in total is available with respect to the previous H.E.S.S. observations [15].

In this Letter, we report on a new search for DM annihilation in the central region of the Milky Way halo using an unprecedented dataset from very-high-energy (VHE, $E \gtrsim 100 \text{ GeV}$) observations taken with the five-telescope H.E.S.S. array of the Galactic Center region.

Observations and data analysis.—The H.E.S.S. Collaboration is carrying out an extensive observation program to survey the central region of the Milky Way. Such a region can be observed with the H.E.S.S. observatory under very good conditions due to its location near the tropic of Capricorn. The survey aims at covering the inner several hundred parsecs of the Galactic Center region, in order to achieve the best possible sensitivity for DM annihilation signals and Galactic Center outflows. Such a survey, hereafter referred to as the Inner Galaxy Survey (IGS), is the first-ever conducted deep VHE γ -ray survey of the Galactic Center region. In order to cover so far unexplored regions in VHE gamma rays, the current implementation of the IGS is based on the definition of a grid of telescope pointing positions up to Galactic latitudes $b = +3.2^\circ$, as shown in the top-left panel of Fig. 1 of Ref. [15]. The present dataset makes use of 28-min data taking runs between 2014 and 2020, amounting to a total of 546 h (live time) of high-quality data following the standard data quality selection procedure [24]. Observations are taken at observational zenith angles lower than 40° to minimize systematic uncertainties in the event reconstruction. The observational campaign results in an averaged observational zenith angle of 18° for the present dataset. An acceptance-corrected exposure time of at least 10 h is reached up to $b \approx +6^\circ$ with the present dataset. γ -ray-like events are selected and reconstructed with a semianalytical shower model technique based on a fit of observed shower images to a semi-analytical shower model [25]. An angular resolution of 0.06° (68% containment radius) and an energy resolution of 10% above 200 GeV are achieved. The central region of the Milky Way is a complex environment including numerous regions with VHE γ -ray emission [26–28] as well as varying night sky background in the field of view [14]. A study of the systematic uncertainties in the background determination is presented in Ref. [15].

The DM annihilation signal is searched in regions of interest (ROI) defined as rings centered on the nominal GC position. In order to avoid γ -ray contamination from known astrophysical sources in the whole field of view, a conservative set of exclusion regions is defined (see Fig. 1 in Ref. [15]) according to the H.E.S.S. angular resolution and the extension of the emissions in the field of view. See Ref. [15] for more details. The ROIs are therefore considered with inner radii from 0.5° to 2.9° , and width of 0.1° each. This set of 25 rings is hereafter referred as to the ON region. For each ROI, the residual γ -ray background is measured on a run-by-run basis in a region of the field of view taken symmetrically to the ON region from the pointing position, which is hereafter referred to as the OFF region. The excluded regions are similarly removed from the ON and OFF regions such that they keep the same solid angle and acceptance. The OFF regions are always sufficiently far away from the ON regions, such that a significant difference in the expected DM signal between ON and OFF regions is obtained. More details are provided in Fig. 2 of Ref. [15]. Any potential unaccounted γ -ray emission is considered as part of the measured excess, which makes the analysis conservative as long as no signal is detected.

For each ROI, event distributions are built as a function of energy and are hereafter referred to as the energy count distributions. The systematic uncertainty on the normalization of the measured energy count distributions is 1% [15].

The statistical data analysis is based on a two-dimensional log-likelihood ratio test statistic which makes use of the expected spectral and spatial DM signal features in 67 logarithmically spaced energy bins and 25 spatial bins corresponding to the ROI. For a given DM mass, the likelihood function reads

$$\begin{aligned} \mathcal{L}_{ij}(\mathbf{N}^S, \mathbf{N}^B | \mathbf{N}_{\text{ON}}, \mathbf{N}_{\text{OFF}}) &= \frac{[\beta_{ij}(N_{ij}^S + N_{ij}^B)]^{N_{\text{ON},ij}} e^{-\beta_{ij}(N_{ij}^S + N_{ij}^B)}}{N_{\text{ON},ij}!} \\ &\times \frac{[\beta_{ij}(N_{ij}^{S'} + N_{ij}^{B'})]^{N_{\text{OFF},ij}} e^{-\beta_{ij}(N_{ij}^{S'} + N_{ij}^{B'})}}{N_{\text{OFF},ij}!} \\ &\times e^{\frac{(1-\beta_{ij})^2}{2\sigma_{\beta_{ij}}^2}}. \end{aligned} \quad (2)$$

$N_{\text{ON},ij}$ and $N_{\text{OFF},ij}$ are the number of measured events in the ON and OFF regions, respectively, in the spectral bin i and in the spatial bin j . N_{ij}^B is the expected number of background events in the (i, j) bin for the ON and OFF regions. N_{ij}^S and $N_{ij}^{S'}$ are the total number of DM events in the (i, j) bin for the ON and OFF regions, respectively. It is obtained by folding the expected DM flux given in Eq. (1) with the energy-dependent acceptance and energy resolution. The γ -ray yield $dN_{\gamma}^f/dE_{\gamma}$ in the channel f is computed with the Monte Carlo event collision generator

PYTHIAv8.135, including final state radiative corrections [29]. The J factor values of each ROI are reported in Table III of Ref. [15]. $N_{ij}^S + N_{ij}^B$ is the total number of events in the spatial bin j and spectral bin i . The systematic uncertainty can be accounted for in the likelihood function as a Gaussian nuisance parameter where β_{ij} acts as a normalization factor and $\sigma_{\beta_{ij}}$ is the width of the Gaussian function (see, for instance, Refs. [30–32]). β_{ij} is found by maximizing the likelihood function such that $d\mathcal{L}_{ij}/d\beta_{ij} \equiv 0$. A value of 1% for $\sigma_{\beta_{ij}}$ is used [15].

In case of no significant excess in the ROIs, constraints on $\langle\sigma v\rangle$ are obtained from the log-likelihood ratio TS described in Ref. [33] assuming a positive signal $\langle\sigma v\rangle > 0$ [15]. We used the high statistics limit in which the TS follows a χ^2 distribution with one degree of freedom. Values of $\langle\sigma v\rangle$ for which TS is higher than 2.71 are excluded at the 95% confidence level (CL).

Results.—We find no significant excess in any of the ON regions with respect to the OFF regions. An analysis crosscheck performed using independent event calibration and reconstruction [34] corroborates the absence of significant excess. Hence, we derive 95% CL upper limits on $\langle\sigma v\rangle$. We explore the self-annihilation of WIMPs with masses from 200 GeV up to 70 TeV, into the quark ($b\bar{b}$, $t\bar{t}$), gauge bosons (W^+W^- , ZZ), lepton (e^+e^- , $\mu^+\mu^-$, $\tau^+\tau^-$), and Higgs (hh) channels, respectively.

Figure 1 shows the 95% CL observed and expected upper limits for the W^+W^- and $\tau^+\tau^-$ channels, respectively, for the above-mentioned Einasto profile.

The observed limits are computed with ON and OFF measured event distributions. The expected limits are obtained from 300 Poisson realizations of the background extracted from the OFF regions. See Supplement Material [15] for more details. The mean expected upper limit and the 68% and 95% containment bands are plotted. The 95% CL observed limits reach $3.7 \times 10^{-26} \text{ cm}^3 \text{ s}^{-1}$ for a DM particle mass of 1.5 TeV in the W^+W^- channel, and $1.2 \times 10^{-26} \text{ cm}^3 \text{ s}^{-1}$ for 0.7 TeV DM mass in the $\tau^+\tau^-$ annihilation channel. The limits in the $\tau^+\tau^-$ annihilation channel cross the $\langle\sigma v\rangle$ values expected for DM particles annihilating with thermal-relic cross section [35]. The limits for the other annihilation channels are shown in Fig. 3 of Ref. [15]. At 1.5 TeV DM mass, we obtain an improvement factor of 1.6 with respect to the results shown in Ref. [13]. The larger statistics of the dataset from longer observational live time and the data taking with the CT1-5 array of H.E.S.S. contribute to the higher sensitivity of the present analysis.

The left panel of Fig. 2 shows the limits for the NFW profile as well as an alternative set of parameters for the Einasto profile described in Ref. [29]. Assuming a kiloparsec-sized cored DM density distribution such as the Burkert profile would weaken the limits by about 2 orders of magnitude, while a Moore-like profile would improve the limit by a factor of about 2.

The right panel of Fig. 2 summarizes the limits obtained from 254 h of previous H.E.S.S. observation of the Galactic Center [13], from the HAWC observation of the Galactic Center [36], from the observation of 15 dwarf galaxy

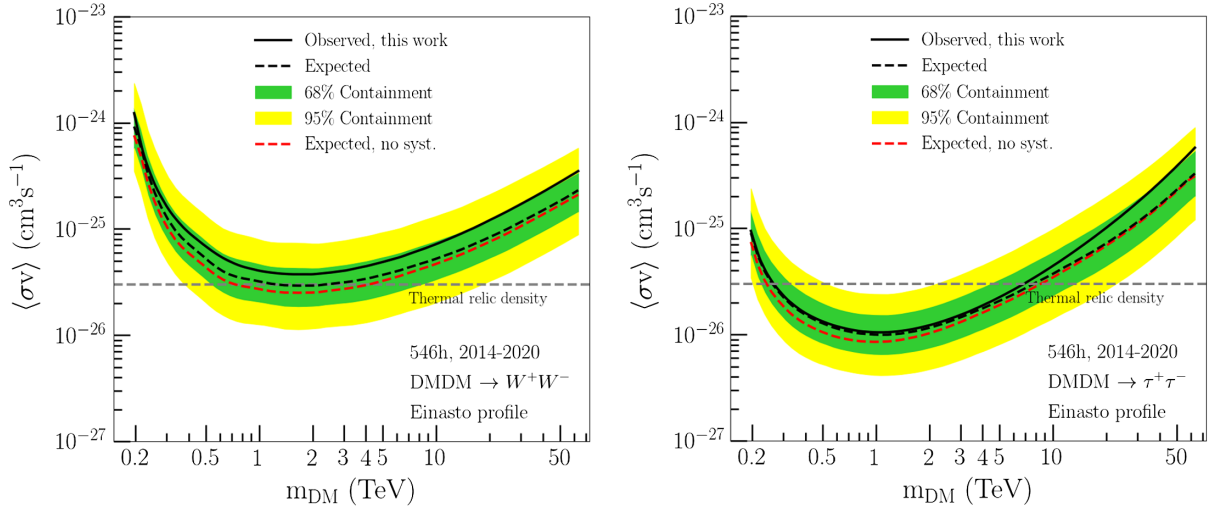


FIG. 1. Constraints on the velocity-weighted annihilation cross section $\langle\sigma v\rangle$ for the W^+W^- (left panel) and $\tau^+\tau^-$ (right panel) channels derived from the H.E.S.S. observations taken from 2014 to 2020. The constraints are expressed as 95% CL upper limits including the systematic uncertainty on $\langle\sigma v\rangle$ as a function of the DM mass m_{DM} . The observed limit is shown as a black solid line. The mean expected limit (black dashed line) together with the 68% (green band) and 95% (yellow band) CL statistical containment bands are shown. The mean expected upper limit without systematic uncertainty is also shown (red dashed line). The horizontal gray long-dashed line is set to the value of the natural scale expected for the thermal-relic WIMPs. The constraints obtained in the $b\bar{b}$, $t\bar{t}$, ZZ , hh , $\mu^+\mu^-$, and e^+e^- channels are given in Fig. 3 of Ref. [15].

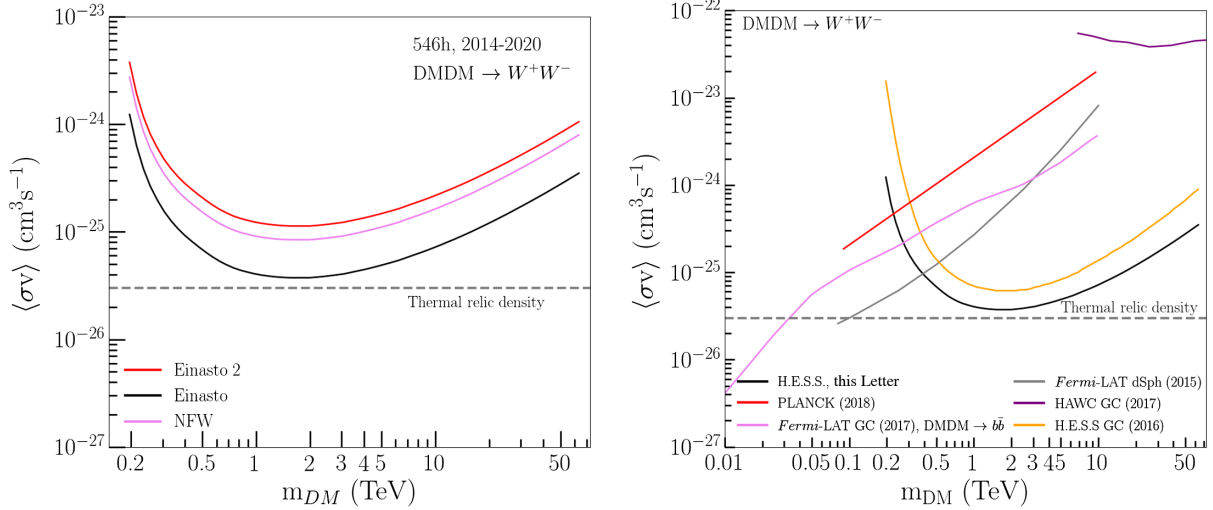


FIG. 2. Left panel: Impact of the DM density distribution on the constraints on the velocity-weighted annihilation cross section $\langle\sigma v\rangle$. The constraints expressed in terms of 95% CL upper limits including the systematic uncertainty, are shown as a function of the DM mass m_{DM} in the W^+W^- channel for the Einasto profile (black line), another parametrization of the Einasto profile [29] referred as to Einasto 2 (red line), and the NFW profile (pink line), respectively. Right panel: Comparison of present constraints in the W^+W^- channel with the previous published H.E.S.S. limits from 254 h of observations of the GC [13] (orange line), the limits from the observation of the GC with HAWC [36] (purple line), the limits from the observations of 15 dwarf galaxy satellites of the Milky Way by the Fermi satellite [37] (gray line), the limits from the cosmic microwave background with PLANCK [2] (red line). The limits from the observation of the GC with the Fermi satellite in the $b\bar{b}$ channel [38] are also shown (violet line). The Einasto profile is used for GC observations.

satellites of the Milky Way [37] as well as from the observation of the GC with *Fermi*-LAT [38], and the limits from the cosmic microwave background measured by PLANCK [2]. The present H.E.S.S. constraints surpass the *Fermi*-LAT limits for particle masses above ~ 300 GeV.

Summary.—In this Letter we report on the latest results on a search for annihilating DM signals from new observations of the inner halo of the Milky Way with the H.E.S.S. five-telescope array. The present dataset amounts to 546 h of total live time spread over 6 yr of H.E.S.S. observations. The absence of significant excess yields constraints on the velocity-weighted annihilation cross section of Majorana WIMPs. In the W^+W^- channel we obtain 95% CL upper limits of $3.7 \times 10^{-26} \text{ cm}^3 \text{ s}^{-1}$ for DM particles with mass of 1.5 TeV, assuming an Einasto profile. These new limits improve significantly upon the previous constraints and are the most constraining so far in the TeV mass range. The strongest limits are obtained for the $\tau^+\tau^-$ channel, reaching $1.2 \times 10^{-26} \text{ cm}^3 \text{ s}^{-1}$, for a DM particle mass of 0.7 TeV. The limits obtained in the $\tau^+\tau^-$ and e^+e^- channels challenge natural $\langle\sigma v\rangle$ values expected for the thermal-relic WIMPs in the TeV DM mass range. The observations carried out with the IGS program as well as the use of the full five-telescope array contribute to the improved sensitivity of this analysis. VHE observations of the central region of the Milky Way with IACTs such as H.E.S.S. are unique for an in-depth study of WIMP models and provide a crucial insight of the TeV WIMP DM paradigm. They provide an

unprecedented dataset to explore the yet-uncharted parameter space of multi-TeV DM models such as the benchmark candidates Wino and Higgsino (see, for instance, Ref. [39] and references therein) which naturally arise in simple extensions to the standard model. The IGS program carried out with H.E.S.S. is an important legacy of H.E.S.S. and paves the way to future Southern-site observations with CTA [32].

The support of the Namibian authorities and of the University of Namibia in facilitating the construction and operation of H. E. S. S. is gratefully acknowledged, as is the support by the German Ministry for Education and Research (BMBF), the Max Planck Society, the German Research Foundation (DFG), the Helmholtz Association, the Alexander von Humboldt Foundation, the French Ministry of Higher Education, Research and Innovation, the Centre National de la Recherche Scientifique (CNRS/IN2P3 and CNRS/INSU), the Commissariat à l'énergie atomique et aux énergies alternatives (CEA), the U.K. Science and Technology Facilities Council (STFC), the Knut and Alice Wallenberg Foundation, the Polish Ministry of Education and Science, Agreement No. 2021/WK/06, the South African Department of Science and Technology and National Research Foundation, the University of Namibia, the National Commission on Research, Science & Technology of Namibia (NCRST), the Austrian Federal Ministry of Education, Science and Research and the Austrian Science Fund (FWF), the Australian Research Council (ARC), the Japan Society for the Promotion of

Science and by the University of Amsterdam. We appreciate the excellent work of the technical support staff in Berlin, Zeuthen, Heidelberg, Palaiseau, Paris, Saclay, Tübingen and in Namibia in the construction and operation of the equipment. This work benefitted from services provided by the H. E. S. S. Virtual Organisation, supported by the national resource providers of the EGI Federation.

*Corresponding authors.

contact.hess@hess-experiment.eu

- [1] P. A. R. Ade *et al.* (Planck Collaboration), Planck 2015 results. XIII. Cosmological parameters, *Astron. Astrophys.* **594**, A13 (2016).
- [2] N. Aghanim *et al.* (Planck Collaboration), Planck 2018 results. VI. Cosmological parameters, *Astron. Astrophys.* **641**, A6 (2020); **652**, C4(E) (2021).
- [3] J. Silk *et al.*, *Particle Dark Matter: Observations, Models and Searches*, edited by G. Bertone (Cambridge University Press, Cambridge, England, 2010).
- [4] J. L. Feng, Dark matter candidates from particle physics and methods of detection, *Annu. Rev. Astron. Astrophys.* **48**, 495 (2010).
- [5] L. Roszkowski, E. M. Sessolo, and S. Trojanowski, WIMP dark matter candidates and searches: current status and future prospects, *Rep. Prog. Phys.* **81**, 066201 (2018).
- [6] G. Jungman, M. Kamionkowski, and K. Griest, Supersymmetric dark matter, *Phys. Rep.* **267**, 195 (1996).
- [7] F. Kahlhoefer, Review of LHC dark matter searches, *Int. J. Mod. Phys. A* **32**, 1730006 (2017).
- [8] M. Schumann, Direct detection of WIMP dark matter: Concepts and status, *J. Phys. G* **46**, 103003 (2019).
- [9] L. E. Strigari, Dark matter in dwarf spheroidal galaxies and indirect detection: A review, *Rep. Prog. Phys.* **81**, 056901 (2018).
- [10] A. M. Ghez *et al.*, Measuring distance and properties of the milky way's central supermassive black hole with stellar orbits, *Astrophys. J.* **689**, 1044 (2008).
- [11] V. Springel, S. D. M. White, C. S. Frenk, J. F. Navarro, A. Jenkins, M. Vogelsberger, J. Wang, A. Ludlow, and A. Helmi, A blueprint for detecting supersymmetric dark matter in the Galactic halo, *Nature (London)* **456**, 73 (2008).
- [12] J. F. Navarro, C. S. Frenk, and S. D. M. White, A Universal density profile from hierarchical clustering, *Astrophys. J.* **490**, 493 (1997).
- [13] H. Abdallah *et al.* (H.E.S.S. Collaboration), Search for Dark Matter Annihilations Towards the Inner Galactic Halo from 10 Years of Observations with H.E.S.S., *Phys. Rev. Lett.* **117**, 111301 (2016).
- [14] H. Abdallah *et al.* (H.E.S.S. Collaboration), Search for Gamma-Ray Line Signals from Dark Matter Annihilations in the Inner Galactic Halo from 10 Years of Observations with H.E.S.S., *Phys. Rev. Lett.* **120**, 201101 (2018).
- [15] See Supplemental Material at <http://link.aps.org/supplemental/10.1103/PhysRevLett.129.111101> for more details, which includes Ref. [16].
- [16] A. Abramowski *et al.* (H.E.S.S. Collaboration), Search for a Dark Matter annihilation signal from the Galactic Center halo with H.E.S.S., *Phys. Rev. Lett.* **106**, 161301 (2011).
- [17] R. Catena and P. Ullio, A novel determination of the local dark matter density, *J. Cosmol. Astropart. Phys.* **08** (2010) 004.
- [18] J. I. Read, The local dark matter density, *J. Phys. G* **41**, 063101 (2014).
- [19] Estimates of the local DM density show an uncertainty of about a factor of 2 [20].
- [20] P. Zyla *et al.* (Particle Data Group), Review of particle physics, *Prog. Theor. Exp. Phys.* **2020**, 083C01 (2020), and 2021 update.
- [21] A. Burkert, The Structure of dark matter halos in dwarf galaxies, *Astrophys. J. Lett.* **447**, L25 (1995).
- [22] J. Diemand, B. Moore, and J. Stadel, Convergence and scatter of cluster density profiles, *Mon. Not. R. Astron. Soc.* **353**, 624 (2004).
- [23] A. Abramowski *et al.* (H.E.S.S. Collaboration), Constraints on an Annihilation Signal from a Core of Constant Dark Matter Density around the Milky Way Center with H.E.S.S., *Phys. Rev. Lett.* **114**, 081301 (2015).
- [24] F. Aharonian *et al.* (H.E.S.S. Collaboration), Observations of the Crab Nebula with H.E.S.S., *Astron. Astrophys.* **457**, 899 (2006).
- [25] M. de Naurois and L. Rolland, A high performance likelihood reconstruction of gamma rays for imaging atmospheric Cherenkov telescopes, *Astropart. Phys.* **32**, 231 (2009).
- [26] F. Aharonian *et al.* (H.E.S.S. Collaboration), Spectrum and variability of the Galactic center VHE gamma-ray source HESS J1745-290, *Astron. Astrophys.* **503**, 817 (2009).
- [27] A. Abramowski *et al.* (H.E.S.S. Collaboration), Acceleration of petaelectronvolt protons in the Galactic Centre, *Nature (London)* **531**, 476 (2016).
- [28] H. Abdalla *et al.* (H.E.S.S. Collaboration), The H.E.S.S. Galactic plane survey, *Astron. Astrophys.* **612**, A1 (2018).
- [29] M. Cirelli, G. Corcella, A. Hektor, G. Hütsi, M. Kadastik, P. Panci, M. Raidal, F. Sala, and A. Strumia, PPC 4 DM ID: A poor particle physicist cookbook for dark matter indirect detection, *J. Cosmol. Astropart. Phys.* **03** (2011) 051.
- [30] H. Silverwood, C. Weniger, P. Scott, and G. Bertone, A realistic assessment of the CTA sensitivity to dark matter annihilation, *J. Cosmol. Astropart. Phys.* **03** (2015) 055.
- [31] V. Lefranc, E. Moulin, P. Panci, and J. Silk, Prospects for annihilating dark matter in the inner galactic halo by the Cherenkov telescope array, *Phys. Rev. D* **91**, 122003 (2015).
- [32] E. Moulin, J. Carr, J. Gaskins, M. Doro, C. Farnier, M. Wood, and H. Zechlin, Science with the Cherenkov Telescope Array: Dark matter programme, in *Science with the Cherenkov Telescope Array* (World Scientific, Singapore, 2019), pp. 45–81.
- [33] G. Cowan, K. Cranmer, E. Gross, and O. Vitells, Asymptotic formulae for likelihood-based tests of new physics, *Eur. Phys. J. C* **71**, 1554 (2011).
- [34] R. D. Parsons and J. A. Hinton, A Monte Carlo template based analysis for Air-Cherenkov arrays, *Astropart. Phys.* **56**, 26 (2014).
- [35] G. Bertone, D. Hooper, and J. Silk, , *Phys. Rep.* **405**, 279 (2005).

- [36] A. Abeysekara *et al.* (HAWC Collaboration), A search for dark matter in the galactic halo with HAWC, *J. Cosmol. Astropart. Phys.* **02** (2018) 049.
- [37] M. Ackermann *et al.* (Fermi-LAT Collaboration), Searching for Dark Matter Annihilation from Milky Way Dwarf Spheroidal Galaxies with Six Years of Fermi Large Area Telescope Data, *Phys. Rev. Lett.* **115**, 231301 (2015).
- [38] M. Ackermann *et al.* (Fermi-LAT Collaboration), The Fermi galactic center GeV excess and implications for dark matter, *Astrophys. J.* **840**, 43 (2017).
- [39] L. Rinchuso, O. Macias, E. Moulin, N. L. Rodd, and T. R. Slatyer, Prospects for detecting heavy WIMP dark matter with the Cherenkov Telescope Array: The Wino and Higgsino, *Phys. Rev. D* **103**, 023011 (2021).